Transactions of the Royal Society of Edinburgh: Earth Sciences, **83**, 127–138, 1992

The Layos Granite, Hercynian Complex of Toledo (Spain): an example of parautochthonous restite-rich granite in a granulitic area

L. Barbero and C. Villaseca

ABSTRACT: The Layos Granite forms elongated massifs within the Toledo Complex of central Spain. It is late-tectonic with respect to the F2 regional phase and simultaneous with the metamorphic peak of the region, which reached a maximum temperature of 800–850°C and pressures of 400–600 MPa. Field studies indicate that this intrusion belongs to the "regional migmatite terrane granite" type. This granite is typically interlayered with sill-like veins and elongated bodies of cordierite/garnet-bearing leucogranites. Enclaves are widespread and comprise restitic types (quartz lumps, biotite, cordierite and sillimanite-rich enclaves) and refractory metamorphic country-rocks including orthogneisses, amphibolites, quartzites, conglomerates and calc-silicate rocks.

These granites vary from quartz-rich tonalites to melamonzogranites and define a S-type trend on a QAP plot. Cordierite and biotite are the mafic phases of the rocks. The particularly high percentage of cordierite (10%–30%) varies inversely with the silica content. Sillimanite is a common accessory mineral, always included in cordierite, suggesting a restitic origin. The mineral chemistry of the Layos Granite is similar to that of the leucogranites and country-rock peraluminous granulites (kinzigites), indicating a close approach to equilibrium. The uniform composition of plagioclase (An_{25}), the high albitic content of the K-feldspar, the continuous variation in the Fe/Mg ratios of the mafic minerals, and the high Ti content of the biotites (2·5–6·5%) suggest a genetic relationship.

Geochemically, the Layos Granite is strongly peraluminous. Normative corundum lies between 4% and 10% and varies inversely with increase in SiO_2. The CaO content is typically low (<1·25%) and shows little variation; similarly the LILE show a limited range. On many variation diagrams, linear trends from peraluminous granulites to the Layos Granite and associated leucogranite can be observed. The chemical characteristics argue against an igneous fractionation or fusion mechanism for the diversification of the Layos Granite. A restite unmixing model between a granulitic pole (represented by the granulites of the Toledo Complex) and a minimum melt (leucogranites) could explain the main chemical variation of the Layos Granite. Melting of a pelitic protolith under anhydrous conditions (biotite dehydration melting) could lead to minimum-temperature melt compositions and a strongly peraluminous residuum.

For the most mafic granites (61–63% SiO_2), it is estimated that the trapped restite component must have been around 65%. This high proportion of restite is close to the estimated rheological critical melt fraction, but field evidence suggests that this critical value has been exceeded. This high restite component implies high viscosity of the melt which, together with the anhydrous assemblage of the Layos Granite and the associated leucogranites, indicates H_2O-undersaturated melting conditions. Under such conditions, the high viscosity magma (crystal-liquid mush) had a restricted movement capacity, leading to the development of parautochthonous plutonic bodies.

KEY WORDS: cordierite-rich granites, dry-melting, Iberian Variscan belt, restite-unmixing, source materials, strongly peraluminous.

The Complejo Plutono-Migmatítico de Toledo, hereafter termed the Toledo Complex, forms an E–W elongated block of high-grade metamorphic and plutonic rocks to the S of Toledo in central Spain. It is part of the Centro–Iberian zone of the axial zone of the Hercynian Belt (Julivert *et al.* 1974). To the N, the Toledo Complex is overlain by post-Mesozoic sedimentary deposits and to the S it is bounded by a major listric fault which brings it into contact with low-grade Palaeozoic sediments in which was emplaced a post-tectonic epizonal batholith (Fig. 1).

The Toledo Complex comprises a metamorphic assemblage of presumed pre-Ordovician age, consisting mainly of metapelites with some orthogneisses and minor metapsammites and marbles. The metamorphism has granulitic facies characteristics and is assumed to be Hercynian in age. The granulite terrane exhumation is explained by extensional thinning developed by great listric faults giving rise to a core-complex geometry (Casquet *et al.* 1988). Emplaced in the metamorphic rocks is a syntectonic felsic to mafic suite of igneous rocks (Barbero *et al.* 1990)

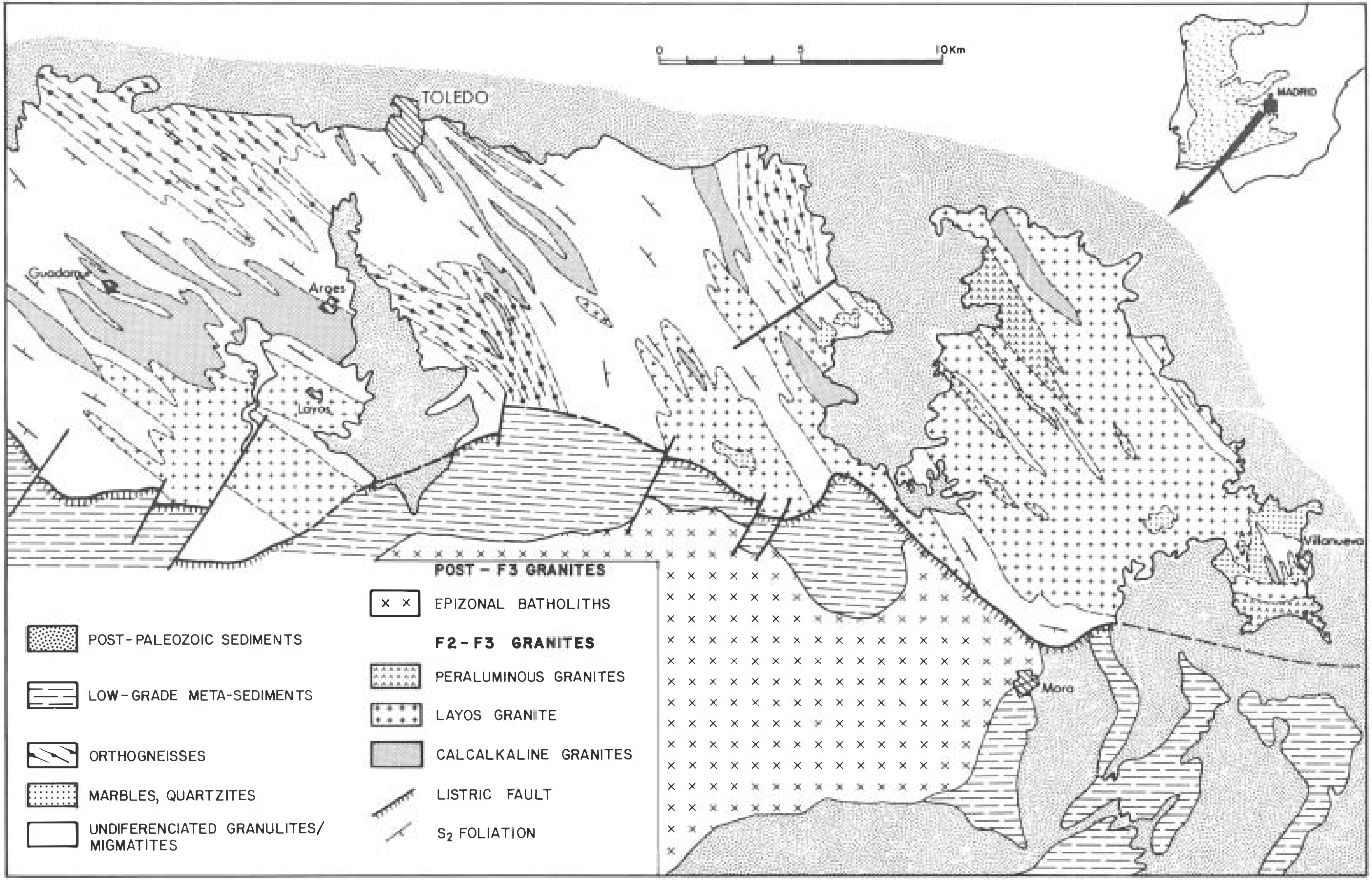

Figure 1 Geological map of the Toledo Complex; inset map indicates the location in the Hercynian Iberian Belt.

which was contemporaneous with or slightly earlier than bodies of heterogeneous strongly peraluminous parautochthonous granites.

This paper deals with petrographical, mineralogical, geochemical and genetic aspects of one of the most peraluminous of these granites, the Layos Granite.

1. Geological setting

The main structure of the Toledo Complex is a strain-slip foliation (S2) with 110°–170° regional strike, usually dipping to the E. This foliation is seen in the metamorphic rocks, mainly in the nonpelitic types (orthogneisses, psammitic paragneisses). In the pelitic varieties, the migmatisation event has erased the S2 foliation and has generated granoblastic non-foliated rocks with a marked banded structure coherent with the S2 foliation of the orthogneisses and metapsammites. In general, the F1 tectonic phase is almost completely obliterated and only some sporadic folds surrounded by S2 and axial F1 surfaces affected by S2 can be observed (Martín Escorza & López Martínez 1978). The F3 tectonic phase causes large- to small-scale asymmetric folds with axial surfaces near-vertical and parallel to the S2 foliation. A weak mineral elongation lineation is sporadically developed, but S3 axial surface foliations are not common. There are two later tectonic phases that cause rotation and folding of the pre-existent structures (Martín Escorza & López Martínez 1978).

The metamorphic rocks of the Toledo Complex are of both sedimentary and igneous origin. The main metaigneous types are leucocratic gneisses and augen gneisses. These rocks are similar to those of the Spanish Central System, probably of late-Cambrian or early-Ordovician age (Vialette *et al.* 1987; Wildberg *et al.* 1989). These metaigneous rocks are exposed mainly in the northern part of the complex (Fig. 1). They retain a foliated structure and because of their low mica content are poorly migmatised.

The metasedimentary types include peraluminous granulites (kinzigitic in affinity), biotitic gneisses, quartzites, amphibolites, marbles and conglomerates, the first being the most abundant type. The granulites exhibit a strong migmatitic layering which defines a stromatic structure characterised by a cordierite-rich mesosome (with Qtz + Kfs + Pl + Crd + Bt + Grt + Sp + Sil ± Ilm) which alternates with narrow leucosomes (Fig. 2(A)), varying from garnet- to cordierite-, and to a lesser extent biotite-, bearing leucogranites. Especially noteworthy is the presence of large rounded garnet crystals in the leucosomes that mainly consist of Qtz + Kfs ± Pl (Fig. 2(A)). In general, it is difficult to find melanosomes or mafic rims around the

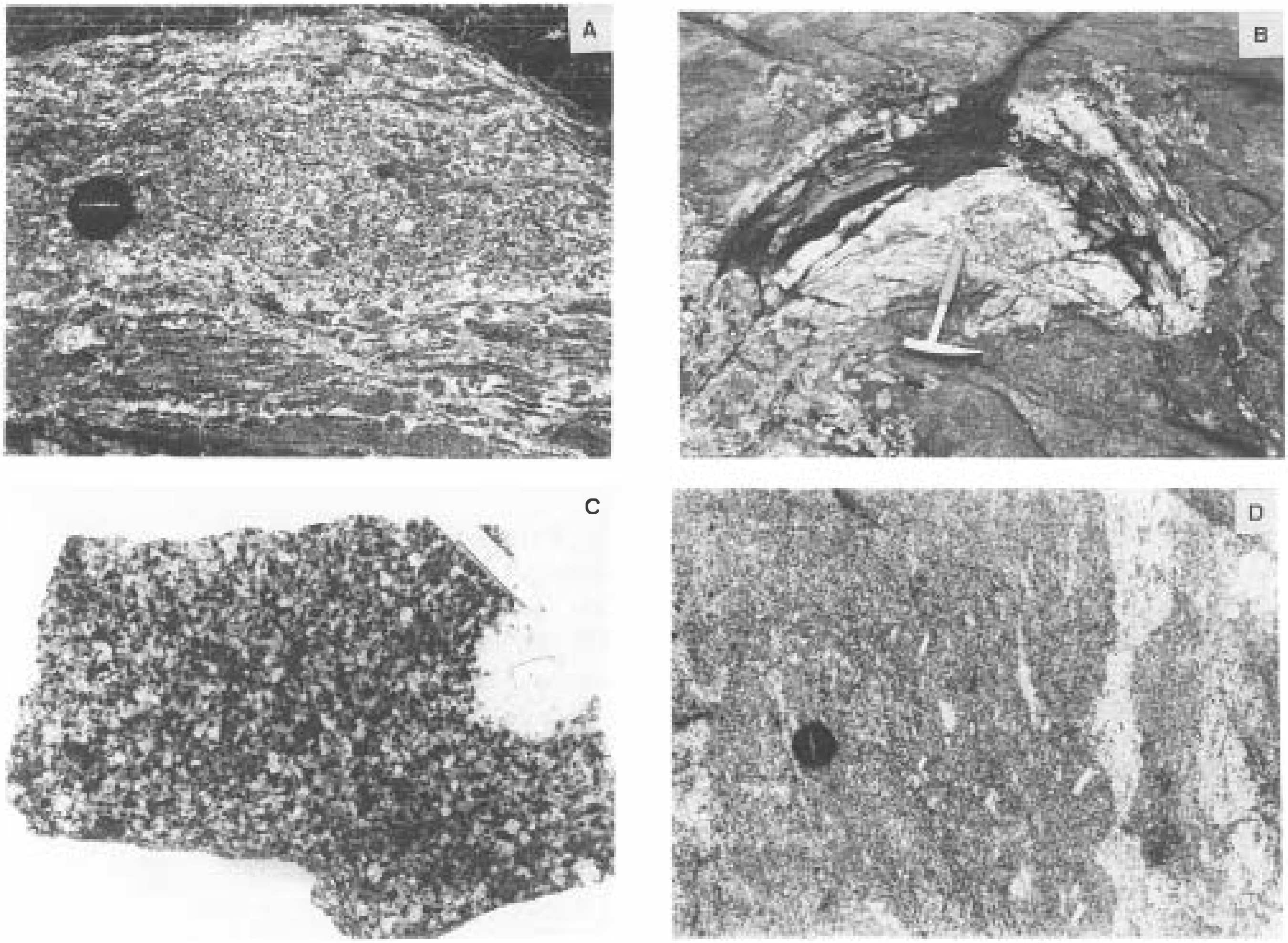

Figure 2 (A) General aspect of the peraluminous migmatitic granulites, showing the stromatic structure marked by the garnet-bearing leucosomes and the cordierite-rich dark mesosome. (B) Partially migmatised enclave of folded metamorphic country rock enclosed in the Layos Granite. (C) Hand-sample aspect of the cordierite-rich Layos Granite; a K-feldspar lump is also shown. (D) Field aspect of the Layos Granite in which it is possible to observe some K-feldspar phenocrysts and also a vein-like associated peraluminous leucogranite.

leucosomes. Sometimes the stromatic structure of the rock is disrupted, leading to diatexitic rocks with similar appearance to the Layos Granite.

Marbles, calc-silicate rocks and quartzites are abundant in the eastern part of the Toledo Complex (Fig. 1). Elsewhere these rocks appear as layers boudinaged and occasionally disrupted in the migmatitic pelites.

Two groups of igneous rocks may be distinguished, namely calcalkine granites and associated mafic rocks, and peraluminous granites (Fig. 1). Both were emplaced relatively late with respect to the second deformational phase; they sometimes show intrusive features and locally cut the S2 foliation. In places it is possible to observe enclaves with early F3 folds enclosed in the granites (Fig. 2(B)). Nevertheless, all the granites show local development of foliation and phenocryst alignment with the S2 direction, and in some places these structures are folded by the third phase (F3). Thus the age of emplacement of these granites must be close to the second tectonic phase, probably between F2 and F3.

The calcalkaline granites and associated mafic rocks comprise three different suites which have been studied by Barbero *et al.* (1990). The first consists of olivine–pyroxene gabbros that outcrop as isolated sills, enclaves and small massifs within the calcalkaline granites. The second consists of amphibole gabbros that are always associated with the intermediate and felsic granites; locally it is possible to observe mingling processes between them. The third suite comprises intermediate–felsic granites, with variable porphyritic texture, in which are typically found microgranular tonalitic enclaves (Barbero *et al.* 1990).

The peraluminous granites form two groups based on the content of normative corundum. Moderately peraluminous granites (normative corundum ≤4%) consist of the Moncloa type, a K-feldspar megacryst-bearing porphyritic granodiorite; the Villanueva type, a garnet-bearing microporphyritic granite; and the Fuente-Topino type, a biotitic leucogranite with cordierite aggregates. Strongly peraluminous granites (normative corundum >4%) are structurally and lithologically heterogeneous and rich in xenoliths and restitic components. To this group belongs the cordierite-bearing Layos Granite which is commonly associated with peraluminous leucogranites, resembling the vein-like types of migmatite leucosomes.

2. Metamorphic grade

The coexistence of the assemblage Grt + Crd + Sil + Bt + Sp + Kfs in pelitic rocks, together with the presence of orthopyroxene in metamorphic coronas around olivine in the gabbros (Barbero & Villaseca 1988) are indicative of granulite facies. The extensive migmatisation and anatexis observed in the pelitic rocks is also consistent with high-grade metamorphic conditions. The coexistence of garnet, biotite and cordierite indicates low-pressure conditions (Green & Ringwood 1967); this is consistent with the absence of garnet in the coronitic gabbros.

The results of several calculations using different mineral equilibria in the peraluminous granulites, biotitic gneisses and metabasites are summarised in Table 1. A maximum pressure limit has been estimated with the GRIPS barometer (Bohlen & Liotta 1986; Ghent & Stout 1984) of around 700 MPa for temperatures near 800°C. The garnet–biotite, cordierite–biotite and spinel–cordierite thermometers yield temperatures between 720 and 870°C. To avoid closure problems with the Fe–Mg interchange thermometers (Frost & Chacko 1989) we have estimated the cross-over of the GASP barometer with other *P–T*-dependent equilibria (e.g. spinel–cordierite). This cross-over indicates temperatures between 770 and 820°C, in agreement with the other temperature estimates, and pressures of 500–600 MPa, clearly under the GRIPS limit.

The formation of cordierite by garnet destabilisation (coronas of cordierite around garnet are frequent in these granulites), gives pressures 50–150 MPa lower than the estimated metamorphic peak conditions, suggesting an isothermal decompression process in the area. This is very frequent in migmatitic Variscan terranes (Ibarguchi & Martínez 1982; Jones & Brown 1990). Temperature estimates in the metamorphic assemblages of the metabasites, based on Opx–Cpx and Opx–Bt thermometers (Table 1), give values between 770–950°C, confirming the granulitic character of the area. In summary, the metamorphic peak conditions of the Toledo Complex are within the range of 800 ± 50°C and 500 ± 100 MPa, clearly in the granulite facies. Under these conditions, biotite breakdown and subsequent dehydration melting reactions can occur; thus the development of granulite facies paragenesis and partial melting are concomitant processes. This coincidence is not fortuitous as in regions which are inferred to have yielded significant quantities of granitic melts by fluid-absent partial fusion, temperature estimates are always restricted to this range of 800–850°C, indicating either a buffering effect and/or the inability of geothermometers to record higher temperatures (Vielzeuf *et al.* 1990).

3. Petrography and mineralogy of the Layos Granite

The Layos Granite has a distinctive dark colour (Fig. 2(C)) due to the high proportion of cordierite, reaching 30% in

Table 1 Peak metamorphic temperatures (°C) and pressure (MPa) estimates from various calibrations

		Temperature							Pressure		
		Grt–Bt		Grt–Crd		Sp–Crd	Opx–Cpx	Opx–Bt	GASP	Sp–Crd	Grt–Crd
Sample	Type	T1	T2	T3	T4						
87085	Granulite	826	841	827	797	868					
T-356	Granulite	807	821	793	762	751			540	610	400
90961	Granulite	774	785	829	799	839			560	590	420
T-361	Gneiss	743	757	722	690	768			620	560	540
89083	Gabbro						903	951			
89081	Gabbro						837				
87075	Gabbro							772			

Notes: All temperature and pressure estimates are based on averaged garnet core, and biotite or cordierite from matrix. Garnet–biotite thermometers are: T1 = Ferry & Spear (1978), T2 = Hodges & Spear (1982); garnet–cordierite thermometers are: T3 = Holdaway & Lee (1977), T4 = Lavrenteva & Perchuck (1981); spinel–cordierite thermometry after Vielzeuf (1983); orthopyroxene–clinopyroxene thermometry after Wells (1977); orthopyroxene–biotite thermometry after Sengupta *et al.* (1990); GASP barometer is calculated at 800°C following the method of Ganguly & Saxena (1984); spinel–cordierite barometry after Vielzeuf (1983); garnet–cordierite barometer of Holdaway & Lee (1977).

the most mafic rocks, with a mean value of 20%. Petrographically it varies from quartz-rich tonalites to melamonzogranites, with granodiorites being the most abundant type. On a QAP plot (Fig. 3) it defines a typical S-type distribution. In places it is possible to observe porphyritic varieties characterised by K-feldspar phenocrysts aligned in 120°–140° directions; locally a gradual transition between porphyritic and non-porphyritic types can be observed. The Layos Granite is little deformed and only a weak mineral elongation or compositional banding is locally observed.

This granite is closely related to peraluminous leucogranites that occur as veins or dyke-like bodies within it, and locally define a banded aspect to the granite (Fig. 2(D)). It is also possible to find synplutonic emplacement processes with other strongly peraluminous varieties, which are indicated by the occurrence of imbrication zones following F3 directions. In these zones the interdigitation processes can produce mingled facies between the Layos Granite and the coeval peraluminous granite.

A major characteristic of the Layos Granite is the abundance of enclaves, which comprise three groups. The first group consists of refractory metamorphic country rock enclaves corresponding to the types already described: orthogneisses, amphibolites, quartzitic conglomerates, calc-silicate rocks and marbles. These enclaves are the most abundant and can reach a maximum size of 2–3 m, although usually they are not greater than 20–25 cm in size (Fig. 2(B)).

The second group consists of restitic enclaves which are, in decreasing order of abundance:

(a) Quartz lumps ranging in size from 1–2 cm up to 50 cm. In some of the larger lumps there is a gneissic partial rim around the quartz, suggesting a derivation from vein quartz in the original metamorphic sequence.

(b) Biotite-bearing enclaves usually 1–2 cm in size and rounded in form. They commonly present biotite-bearing layers alternating with cordierite-sillimanite- and minor spinel-bearing layers, resembling the regional peraluminous granulites.

(c) Cordierite-rich enclaves (1–2 cm) generally formed with intergrowths of cordierite and quartz. Minor biotite and sillimanite are locally present.

(d) Sillimanite-rich enclaves of rounded shape and up to 25 cm in diameter. The aluminosilicate is sometimes included in cordierite or plagioclase crystals with minor biotite, K-feldspar, spinel and quartz.

(e) K-feldspar lumps showing corroded borders and perthitic textures that are locally associated with quartz, forming micro-pegmatitic textures. It is possible to find inclusions of quartz, plagioclase, and minor biotite and sillimanite within these crystals. Exceptionally, they can reach up to 25 cm in diameter, but generally they are 3–4 cm in size. They are occasionally surrounded by a biotite rim (Fig. 2(C)).

The third group consists of mafic igneous enclaves. These enclaves are very scarce and can be found in places where mafic rocks outcrop (Villanueva region, see Fig. 1) and it seems likely that they were incorporated at the emplacement level. Amphibole-biotite-bearing quartz diorites and gabbros are the main types. Scarce microgranular enclaves with quartz, plagioclase, biotite and accessory garnet are also present.

The Layos Granite is a medium-grained rock with a hypidiomorphic texture. Occasionally it shows a porphyritic texture defined by euhedral K-feldspar phenocrysts. The major minerals are quartz, plagioclase, K-feldspar, cordierite and biotite. Accessory minerals include apatite, zircon, monazite, tourmaline, sillimanite, garnet, ilmenite (Ilm_{98}), rutile and iron sulphides. Selected mineral compositions are given in Table 2.

Plagioclase composition ranges between An_{25}–An_{23}. In some samples there is a narrow rim with more albitic composition (An_{12}–An_5). Particularly remarkable is the absence of zoning (variations greater than 3% in An are not observed). Thus, neither calcic cores nor more complex and marked zoning are found, in contrast to the other peraluminous or calc-alkaline allochthonous granites (e.g. Rottura *et al.* 1990; Chappell *et al.* 1987). It is noteworthy that the plagioclase has the same composition over the range from tonalites to monzogranites and is also similar to that of the peraluminous granulites and leucogranites (Fig. 4(A)).

K-feldspar compositions vary between Or_{92} and Or_{71}. Occasionally the K-feldspar crystals display some perthitic veins. Sporadically, sillimanite needles, biotite, plagioclase and quartz are included in these crystals. Like the plagioclase, the K-feldspar of the Layos Granites and those of the peraluminous granulites and leucogranites have similar compositions. The relatively high albitic component of the K-feldspar resembles that obtained for minimum-temperature melts and partially fused pelitic xenoliths (Grapes 1985).

The most abundant ferromagnesian phase is cordierite. This mineral usually occurs as euhedral or subhedral grains, with frequent inclusions of acicular sillimanite, biotite and quartz, suggesting a restitic origin for this mineral (Chappell *et al.* 1987). The Fe/(Fe + Mg) ratios vary from 0·38–0·48; they are close to the ratios displayed by the cordierites of the peraluminous granulites (0·38–0·53) and leucogranites (0·44–0·62). The very low Na + K + Ca contents of these cordierites are characteristic of granulite facies cordierites (Vry *et al.* 1990). According to those authors, the low Na + K + Ca values imply relatively high X_{CO_2} in the cordierite (0·3–0·7). Figure 4 is a Mn vs Na + K + Ca plot on which it is clear that the cordierites of the Layos Granite are Mn-, Ca- and alkali-poor compared to those of the typical peraluminous Hercynian Iberian batholiths (Casillas 1989; Rottura *et al.* 1989; Andonaegui 1990).

Biotite occurs as subhedral crystals with a typical interstitial character (Andonaegui 1990). The relatively high Ti and low Al^{VI} contents are typical of granulite facies biotites (Dymek 1983). These high Ti and Al^{VI} values

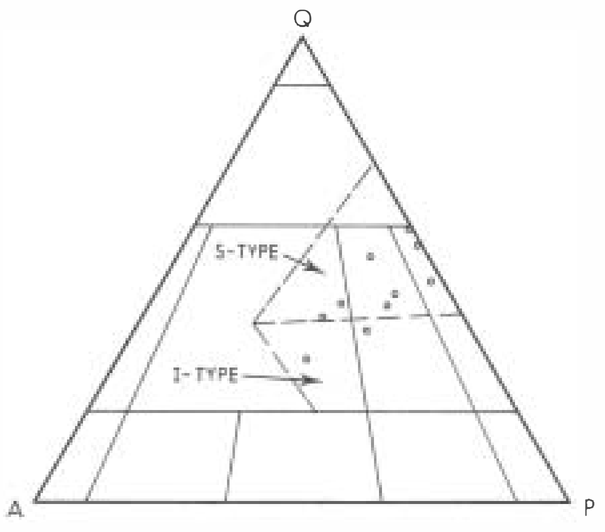

Figure 3 QAP (Streckeisen 1976) plot for selected samples of the Layos Granite; S- and I-type fields after Bowden *et al.* (1984).

Table 2 Representative microprobe analyses of mineral phases of the Layos Granite

	Pl	Kfs	Bt-1	Bt-2	Crd-1	Crd-2	Grt	Ilm
SiO_2	62·51	65·15	34·48	34·93	48·69	48·08	37·41	0·01
TiO_2	0·00	0·01	5·12	3·11	0·00	0·00	0·05	54·19
Al_2O_3	23·18	18·88	16·84	18·18	31·49	31·41	20·28	0·04
FeO*	0·10		19·58	19·82	9·13	10·32	32·37	45·78
Cr_2O_3			0·12	0·00	0·00	0·01	0·04	0·01
MnO				0·08	0·27	0·23	2·50	1·80
MgO			7·84	8·15	6·74	6·68	4·22	0·18
CaO	4·94	0·05	0·04	0·02	0·01	0·00	0·73	0·00
Na_2O	8·86	1·96	0·17	0·08	0·18	0·20		
K_2O	0·26	13·69	9·08	8·99	0·02	0·02		
Total	99·85	99·74	93·27	93·36	96·53	96·95	97·60	102·01
Oxygen	32	32	22	22	18	18	12	3
Si	11·11	11·95	5·39	5·44	5·12	5·07	6·11	0·00
Al(IV)	4·85	4·08	2·61	2·56			0·00	
Al(VI)			0·50	0·78	3·90	3·90	3·90	
Fe	0·01	0·00	2·56	2·58	0·80	0·91	4·42	0·96
Ti			0·40	0·36	0·00	0·00	0·01	1·01
Mn					0·02	0·02	0·35	0·04
Mg			1·83	1·89	1·06	1·05	1·03	0·01
Ca	0·94	0·01	0·01	0·00	0·00	0·00	0·13	
Na	3·05	0·70	0·05	0·02	0·04	0·04		
K	0·06	3·21	1·81	1·78	0·00	0·00		

Notes: Pl = plagioclase, Kfs = K-feldspar; Bt = biotite; Crd = cordierite; Grt = garnet; Ilm = ilmenite.

contrast with the lower values displayed by the biotites of other Variscan peraluminous granites (Fig. 4(C)) (cordierite-bearing granites; Casillas 1989; Andonaegui 1990; Rottura *et al.* 1989). The biotites of the Layos Granite have Fe/(Fe + Mg) ratios very similar to those of the peraluminous granulites, although there is a narrow variation range. This fact suggests a possible restitic origin for this mineral.

Finally, the accessory garnet (Alm_{75} Py_{17} Sp_6 Gr_2) is very low in the spessartine molecule compared to other peraluminous monzogranite–granodiorite plutons (Villaseca & Barbero in press). Similarly, ilmenites are also Mn-poor (≤2·3%) and contrast with the main granitic plutons of the area (Andonaegui 1990; Brandebourger 1984; Casillas 1989), or with the S-type granites (Whalen & Chappell 1988).

In summary, the feldspar and ferromagnesian phases are compositionally different from those of the main peraluminous Hercynian batholiths of the area and from other cordierite-bearing granites (Flood & Shaw 1975; Speer 1981), and define an exotic granitic mineralogical assemblage.

4. Geochemistry of the Layos Granite

Major elements were determined by ICP spectrometry. Trace elements were analysed by XRF spectrometry using the method described by Brändle and Cerqueira (1972). Rare-earth elements were analysed by CNRS (Nancy, France) by ICP spectrometry. Seventeen samples of the Layos Granite from quartz-rich tonalites to monzogranites, six peraluminous granulites and five leucocratic rocks have been analysed. A further 13 analyses of Layos Granite and associated leucogranites are available from Andonaegui (1990). From these 41 analyses we have made a selection of the most significant rock compositions as given in Table 3.

The Layos Granite ranges in SiO_2 content from 61–72%. Most of the samples are clearly richer in modal quartz than the normal granitic series (Fig. 3). The granite is strongly peraluminous with normative corundum values ranging from 4–10%, the mean value being 7%. Normative corundum varies inversely with the silica content. This strongly peraluminous character is also shown on the A–B diagram (Debon & Le Fort 1983), where the Layos Granite defines a strongly positive trend with high A values (Fig. 5); this feature is not very common in other granitic series, and only occurs in some S-type granites (White & Chappell 1987) and some restite-rich types (Clarke & Lyons 1986). On the A–B diagram the most mafic varieties of the Layos Granite plot close to the peraluminous granulites and in the field of pelitic sediment composition (Fig. 5). The felsic members of the Layos Granite trend towards the leucogranitic field. The strongly peraluminous character is in marked contrast with the less peraluminous Iberian Hercynian cordierite-bearing batholiths (normative corundum ≤3%). Furthermore, these allochthonous and post-tectonic plutons show an opposite trend of increase in the peraluminous index with silica content.

The major elements of the Layos Granite show two noteworthy characteristics: firstly, the high Fe, Mg and Ti contents (in some cases $FeO_t + MgO + TiO_2 > 10\%$) reflect the high modal abundance of cordierite and biotite; secondly, the very low variation in the CaO content which precludes igneous fractionation processes involving plagioclase. This limited CaO variation in the Layos Granite is in the same range as in the peraluminous granulites and leucogranites (Fig. 6), and is in accord with the similar plagioclase composition in the three lithological groups.

Similar limited variation, as silica increases, is shown by other major elements and especially the alkalis (Fig. 6). Nevertheless, on Harker Diagrams, the Layos Granite displays linear trends which suggest either mixing between contrasting end-members, or unmixing of some intermediate types into more mafic and felsic end-members. Trace element data display more complex trends (Fig. 6) with generally greater scatter. Nevertheless, some of them show more or less defined ranges of variation. For example, Ba, Rb, Sr and Cr tend to decrease with increasing silica content. The high Cr–Ni content of these granites is controlled by the different proportion of ferromagnesian phases rich in these elements (i.e. biotite, cordierite).

REE patterns of the Layos Granite are characterised by a negative Eu anomaly (Fig. 7); the different samples have similar LREE and more variable HREE patterns ($Gd_N/Lu_N = 0{\cdot}8$–36) than those of the peraluminous granulites. The associated leucogranites have either as much REE as the metasediments or less total REE contents (particularly HREE), with different patterns. The sample with the lowest total REE and the most marked positive Eu anomaly is characteristic of some minimum-temperature granite compositions typical of disequilibrium melting processes in relatively anhydrous environments (Moller & Muecke 1984; Barbey *et al.* 1989) or possibly is the consequence of some crystal accumulation of feldspars (Sawyer 1987).

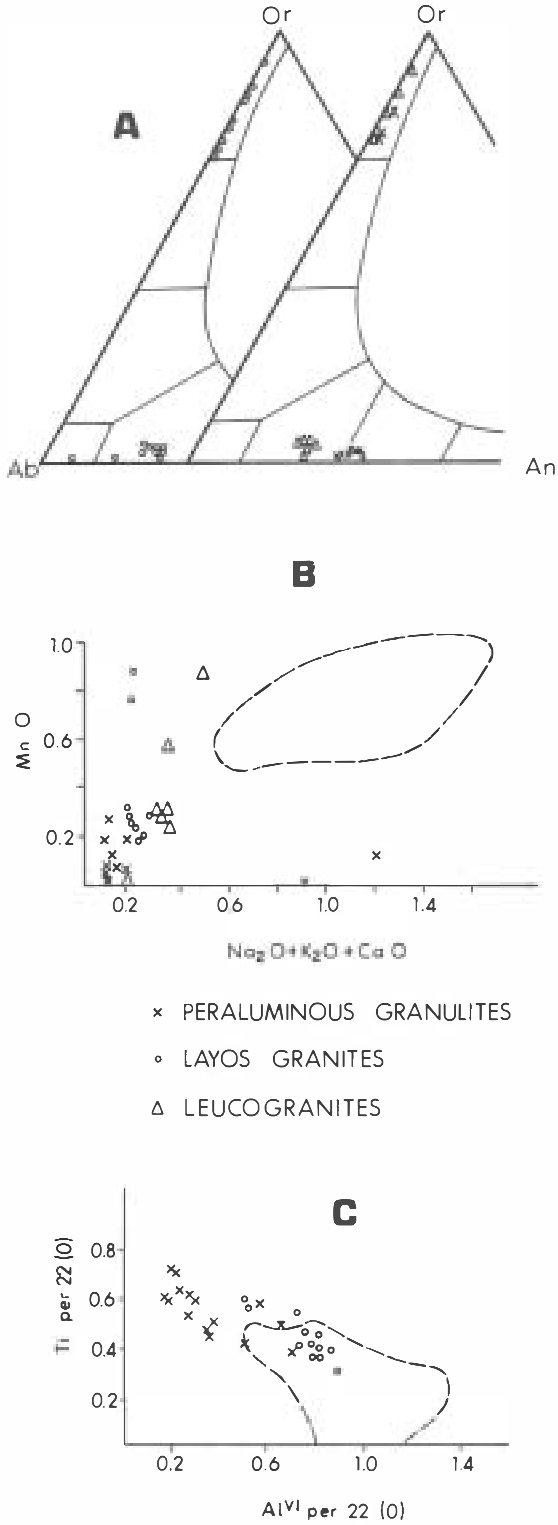

Figure 4 (A) Feldspar compositions on the Or–Ab–An molecular diagram. (B) Cordierite composition on a MnO vs $Na_2O + K_2O + CaO$ plot; dashed field corresponds to cordierites of typical peraluminous Hercynian batholiths. (C) Biotite composition in terms of Ti and Al^{VI} contents; dashed field corresponds to biotites of typical peraluminous Hercynian batholiths (see text for explanation).

5. Granite petrogenesis

5.1. Main evolutionary mechanism

The Layos Granite is a catazonal pluton and a regional-migmatite terrane granite. Its anatectic origin is confirmed by: its parautochthonous character indicated by the absence of a contact aureole in the adjacent metamorphic rocks; the thermodynamical equilibrium between its mineral assemblages and those of the country rock granulites; and the close relationships between the age of emplacement and the migmatisation event.

On many Harker Diagrams the variation trend of the Layos Granite is clearly linear and lies between the compositional fields of granulites and leucogranites (Figs 5, 6). A crystal fractionation process seems to be unlikely

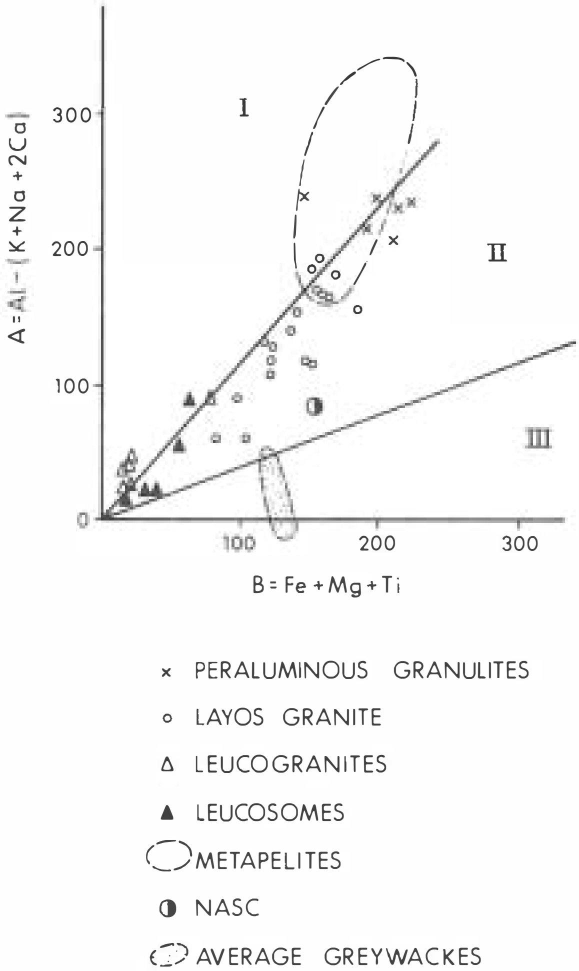

Figure 5 Plot of the peraluminous granulites, Layos Granite and leucogranites in the A–B diagram after Debon & Le Fort (1983); composition fields of metapelites of the Spanish Central System (Villaseca 1983), average greywackes (McRae & Nesbitt 1980) and North American Shale Composite (NASC of Gromet *et al.* 1984) are also reported (see text for explanation); Field I = muscovite > biotite granites; Field II = muscovite ± biotite granites; Field III = muscovite < biotite granites.

Table 3 Major, trace element and corundum normative contents of representative pelitic granulites (1 to 3), Layos Granites (4 to 11) and associated leucogranites (12 to 15); sample 15 is from Andonaegui (1990); sample 12 corresponds to a leucosome band

	1	2	3	4	5	6	7	8	9	10	11	12	13	14	15
Sample	90961	T-383	T-388	89103	90537	91085	90538	90966	90964	90968	89861	T-382	90959	T-400	81925
SiO_2	56·96	57·15	58·19	61·37	63·20	64·61	66·07	68·78	69·82	71·14	72·52	69·50	72·50	74·18	74·36
TiO_2	1·12	1·13	1·12	0·61	0·70	0·82	0·81	0·96	0·53	0·64	0·66	0·52	0·26	0·13	0·06
Al_2O_3	20·10	20·16	19·43	18·45	17·88	15·52	17·03	13·63	14·49	13·44	12·30	14·96	14·81	13·78	14·40
Fe_2O_3	3·11	*9·39	*8·89	1·01	0·19	1·74	0·64	*6·20	1·26	*5·40	0·00	*2·56	0·15	*0·81	0·37
FeO	6·55			5·49	5·79	3·59	5·26		2·47		5·12		0·88		0·75
MgO	3·66	3·39	3·40	2·67	2·38	1·90	2·17	1·70	1·28	1·32	0·29	0·25	0·40		
MnO	0·08	0·08	0·08	0·25	0·07	0·08	0·07	0·06	0·06	0·01	0·00	0·01	0·05		
CaO	1·45	1·54	1·52	0·81	1·22	1·25	1·09	0·76	0·99	1·02	1·01	1·25	1·13		
Na_2O	1·75	1·79	1·82	2·01	2·01	2·61	2·32	2·27	2·71	2·66	3·65	3·25	3·21		
K_2O	2·63	3·90	3·65	4·03	4·27	3·29	3·81	3·65	4·72	2·77	2·77	7·00	5·22	5·34	4·21
P_2O_5	0·20	0·13	0·14	0·23	0·52	0·35	0·23	0·16	0·33	0·19	0·36	0·34	0·28	0·16	0·22
H_2O	1·31	1·06	1·42	2·20	1·42	2·35	1·27	1·51	1·69	1·46	1·10	1·16	0·57	0·64	0·82
Total	98·92	99·72	99·66	99·13	99·65	98·11	100·77	99·68	100·35	99·71	99·75	99·64	99·75	99·79	99·98
Ba	547	762	898	604	839	697	596	663	699	570	278	1174	848	573	614
Cr	541	145	137	364	418	267	427	268	193	390	281	25	20	5	138
Ni	80	57	54	65	45	43	45	38	23	50	37	10	5	5	41
Rb	130	172	136	161	149	127	155	165	169	115	161	263	135	209	79
Sr	187	243	256	173	202	193	192	130	235	151	114	261	197	155	208
Th	16	19	23	16	12	21	7	15	13	9	8	22	12	12	1
Y	35	27	25	23	38	48	25	23	28	18	10	8	9	5	11
Zr	173	218	219	123	195	296	190	309	207	213	198	166	133	71	87
La	61·6	69·4	67·4	33·5			37·6	42·9	32·2	34·0	29·9	50·0	30·8	25·2	
Ce	112·6	135·7	131·8	64·5			71·4	94·2	62·9	74·7	59·8	114·6	60·9	56·0	
Nd	50·9	54·8	54·2	29·1			33·9	42·3	30·0	33·3	28·2	51·3	30·1	20·3	
Sm	10·3	11·0	10·98	6·5			7·5	9·4	7·1	7·6	6·2	11·9	6·3	4·0	
Eu	1·76	1·93	2·09	1·25			1·36	1·40	1·37	1·48	0·90	2·06	1·62	1·01	
Gd	8·23	9·03	8·24	5·43			6·40	7·81	6·64	6·77	4·99	9·65	4·68	3·32	
Dy	6·95	7·07	6·37	4·54			5·55	5·82	5·11	4·96	2·94	3·95	3·95	1·44	
Er	3·34	3·70	3·37	3·05			3·13	3·55	2·76	2·47	1·26	1·14	1·14	0·55	
Yb	3·14	3·30	3·03	4·25			3·22	3·50	3·29	1·99	0·97	0·51	0·51	0·19	
Lu	0·52	0·59	0·58	0·82			0·54	0·63	0·58	0·36	0·17	0·13	0·13	0·07	
C	11·97	11·37	12·41	9·86	8·98	6·23	7·66	5·94	3·91	6·43	3·93	4·28	1·99	0·93	3·03

Notes: * = total Fe as Fe_2O_3.

because of the absence of CaO variation and because an igneous granitic series could not evolve without plagioclase fractionation. However, in the most evolved rocks some porphyritic varieties locally display a gradual transition towards the much more abundant non-porphyritic types, possibly due to limited crystal fractionation. Other processes such as varying degrees of partial melting seem also to be unlikely. In such a fusion process a strong enrichment in incompatible elements and little variation in the compatible ones is to be expected (Minster & Allègre 1977). On incompatible versus compatible element diagrams, the Layos Granite shows little variation for both types of elements, suggesting that a fusion mechanism cannot explain their chemical variability.

Some trace element concentrations in the Layos Granite are quite variable. Zr, P and Th contents show the same variations as in the pelitic granulites, and are always higher than predicted from their solubility in granitic melts at temperatures in the range of this anatectic terrane (Watson 1987). This oversaturation in some HFS elements is better explained by inheritance of zircon, monazite and apatite in the major refractory phases and in the incongruent solids produced in the dehydration melting (biotite, cordierite, garnet, . . .).

The REE contents of the Layos Granite show an inverse variation with silica increase, that is, the more restite-rich a granite, the higher the REE content. This fact again suggests that the accessory phases, which tend to be REE-rich, are mainly of restitic origin or are included in the solid melt residuum (Barbey *et al.* 1990). In general, the Layos Granite has total REE contents intermediate between those of the metapelites and leucogranites. The increase in the La/Lu ratio of the leucogranites with respect to that of the peraluminous granulites and metapelites can be explained by the presence of residual garnet in these rocks, although some of that mineral was consumed in the cordierite-producing reactions.

In view of these observations, we strongly prefer a restite-unmixing process for the origin and diversification of the Layos Granite. In this restite-unmixing model the restitic pole will be represented by the peraluminous granulites, while the minimum-temperature melts correspond to the associated leucogranites.

5.2. Nature of the source

The most likely composition for the source rock would be that of a pelitic sediment. The normative corundum content (>4%), increasing in the less felsic rocks, the low Na2O (≤3%) and CaO contents (≤1·5%), and the LILE content of the Layos Granite (Rb ≈ 100–170 ppm, Sr ≈ 150–250 ppm and Ba ≈ 300–850 ppm), indicate a pelitic parent (Miller 1985). In several geochemical plots, the peraluminous granulites fall in the compositional fields of pelites. In Figure 5 we have plotted the variation field of pelitic metasediments of the Toledo Complex and the Spanish Central System, together with N American Shale Composite (NASC) (Gromet *et al.* 1984), and the mean values of some greywacke sediments (McRae & Nesbitt 1980). It is clear that the peraluminous granulites plot in the pelitic field and far from the other sedimentary rock compositions. Furthermore, on chondrite-normalised spidergrams the Layos Granite and the granulites show similar patterns, with marked negative anomalies in Nb, Sr, P and Ti similar to other S-type granites and pelitic sediments (Thompson *et al.* 1984).

The other pole of the unmixing line corresponds to the leucogranites. We have sampled large leucogranitic massifs and also some leucosomes and little bands. There are some geochemical differences between the leucogranites of the large massifs and those of leucosomes, especially in Na_2O, K_2O, Ba, Rb and Sr (Fig. 6). These differences are also evident in the Qtz–Ab–Or diagram in which the massif-type leucogranites plot close to the theoretical minimum-temperature melt composition in anhydrous conditions, being richer in the Or component than H_2O-saturated melts (Ebadi & Johannes 1991). Some leucosomes are shifted from those thermal minimum compositions. Furthermore, the composition of the leucogranites is similar in major elements to that obtained by experimental melting of metapelitic protoliths (Wickham 1987a; Vielzeuf & Holloway 1988; Patiño & Johnston 1991).

The limited isotopic data on the Layos granodiorite and associated leucogranites (Andonaegui 1990, samples 81942, 81925 and 81926 of table III-6), clearly suggest a crustal source ($^{87}Sr/^{86}Sr \geq 0{\cdot}713$, Fig. 8). The anatectic origin is more evident in the Layos Granite than in other peraluminous Hercynian granites (Del Moro 1987; Andonaegui 1990; Barbero *et al.* 1990; Rottura *et al.* 1990).

5.3. Constraints on melt extraction and emplacement

The available petrographical, mineralogical and geochemical data strongly suggest a restite-unmixing model for the formation of the Layos Granite. An estimate based on the linear patterns on variation diagrams indicates a maximum restitic component of about 65% for the most mafic rocks (SiO_2 61–63%), and about 25–30% for rocks with 67–68% SiO_2. This high proportion of restite in the less evolved types is in good agreement with the observed modal proportion of restitic minerals. Thus, the most mafic rocks have modal cordierite contents of around 30% and about 70% of the quartz may be restitic, although not easily identifiable as such (Chappell *et al.* 1987).

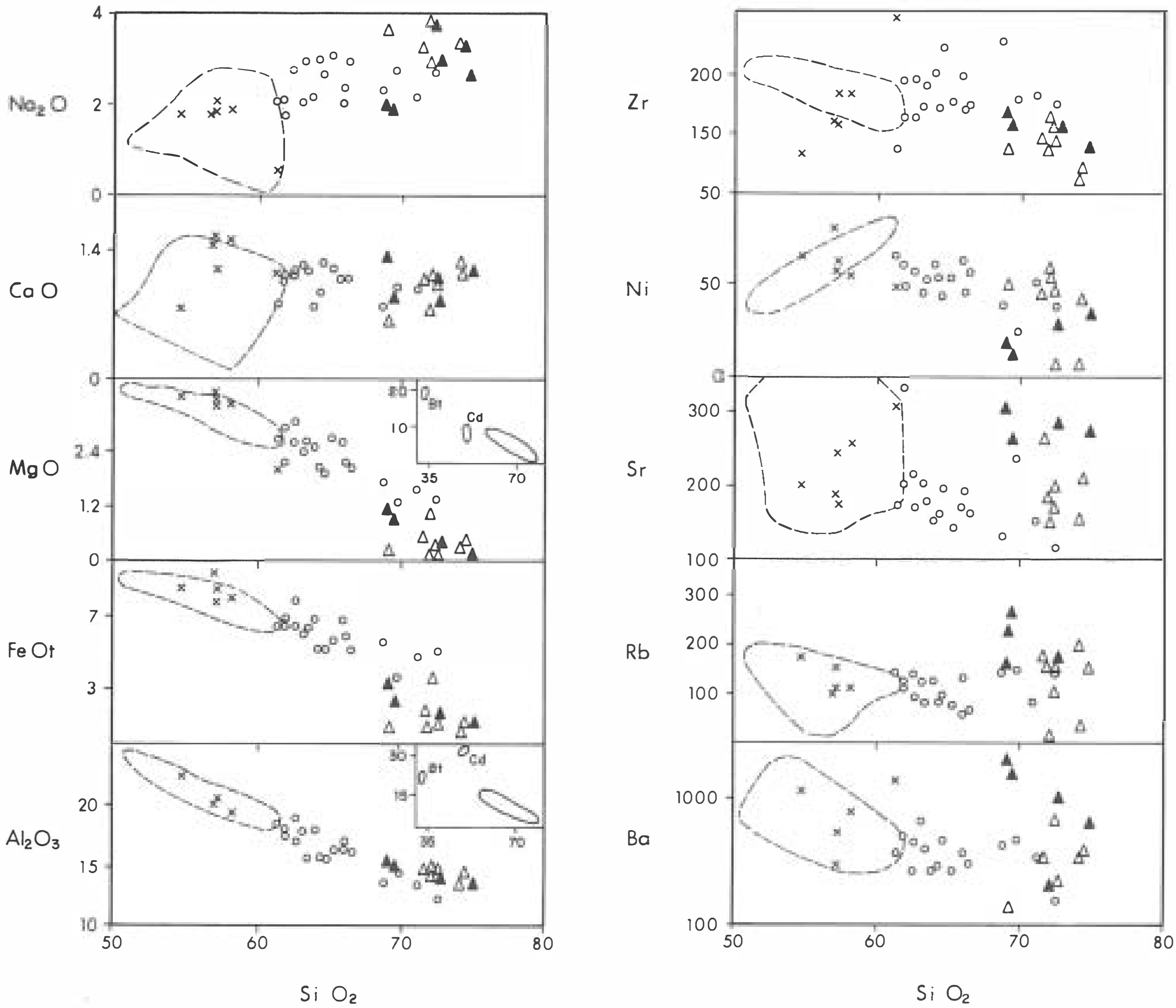

Figure 6 Plots of granulites, Layos Granite and leucogranites in Harker Diagrams; in all diagrams dashed fields represent the compositional variation of the Sierra de Guadarrama metapelites; insets in SiO_2 vs Al_2O_3 and SiO_2 vs MgO diagrams represent the composition of the biotites and cordierites and the variation trend of the Layos Granite (see text for explanation); symbols as in Figure 5.

All these data suggest a melt proportion of between 30% and 60%, always higher than the rheological critical melt fraction. In high strain state conditions, as could be envisaged in the tectonometamorphic climax of the Toledo Complex, segregation would be possible even with as little as 25% high-viscosity H_2O-undersaturated felsic melt (Arzi 1978; Van der Molen & Paterson 1979; Wickham 1987b; Miller *et al.* 1988).

Assuming that the metapelites contain about 25% biotite with 4% H_2O in the biotite and $X_w = 0{\cdot}41$ in the melt, at 800°C and 500 MPa (see Le Breton & Thompson 1988), the amount of melt produced could be around 35% in volume. This value is above the critical melt fraction, and would allow the segregation and accumulation of granitic magma. However, it seems likely that the Layos Granite was never fully melted and that restitic materials (biotite, cordierite, quartz, etc.) were redistributed by mechanical disaggregation due to convective overturn of large (cubic kilometre-sized) partially melted systems (Wickham 1987b). As a crystal-liquid mush, this anhydrous high-viscosity magma had a restricted movement capacity, giving rise to the aforementioned parautochthonous character (Fig. 9).

Other peraluminous magmas generated in this anatectic event contain a lower melt fraction, as represented by near minimum-temperature melt composition (Wickham 1987b). They could be synplutonically segregated as veins or dyke-like bodies within the Layos Granite, and generate a local complex-banded structure (Figs 2, 9).

6. Conclusions

The Toledo Complex consists of high-grade metamorphic rocks which were syntectonically intruded by a mafic–felsic calcalkaline association and by heterogeneous peraluminous granites to which the Layos Granite belongs.

The strongly peraluminous Layos Granite is characterised by a high modal proportion of cordierite and other restitic minerals. Its synchronous emplacement during the regional

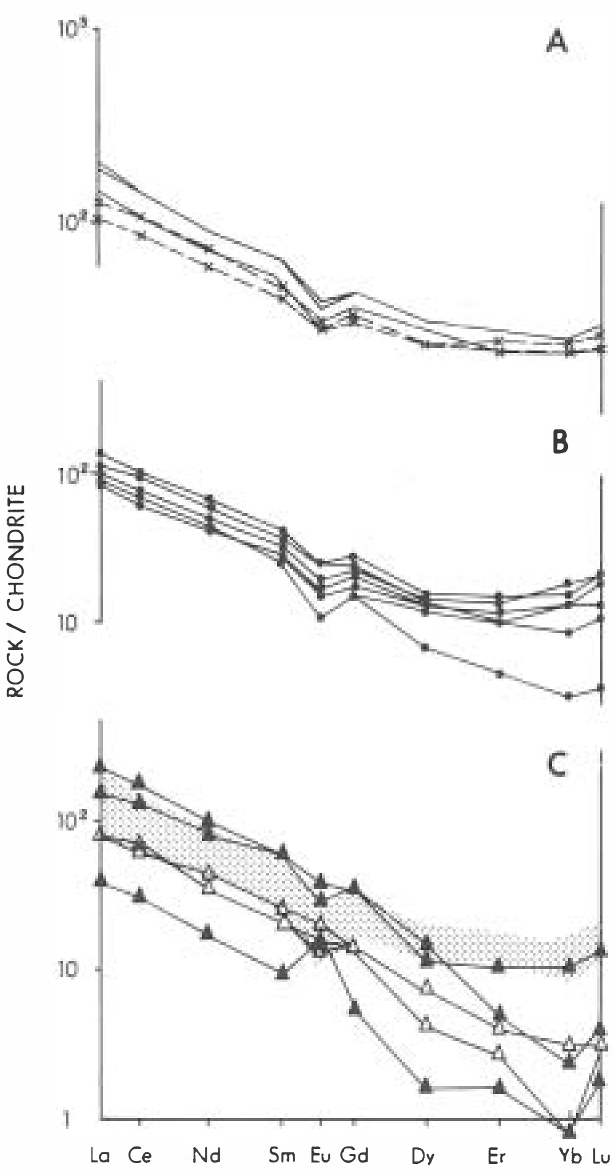

Figure 7 Chondrite-normalised (Masuda *et al.* 1973) REE patterns: (A) Peraluminous granulites (solid line) and metapelites (dashed line); (B) Layos Granite; (C) Leucogranites and leucosomes (solid triangles). The pelitic–granitic variation field (shaded area) is also shown.

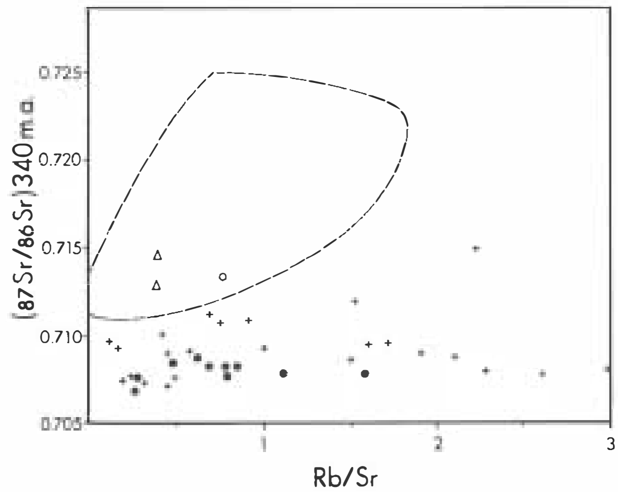

Figure 8 Rb/Sr vs $(^{87}Sr/^{86}Sr)_{340\,M.a.}$ plot showing the leucogranites ($n = 2$) and Layos Granite ($n = 1$); dashed field represents the variation of metapelites from several zones of the Hercynian belt (Ivrea, Strona and Calabria, Del Moro 1987); symbols: circle = Layos granite; triangle = leucogranites; dots = Toledo Complex calcalkaline granites (Barbero *et al.* 1990); crosses = cordierite-bearing Hercynian batholiths (Rottura *et al.* 1990; Andonaegui 1990); see text for explanation.

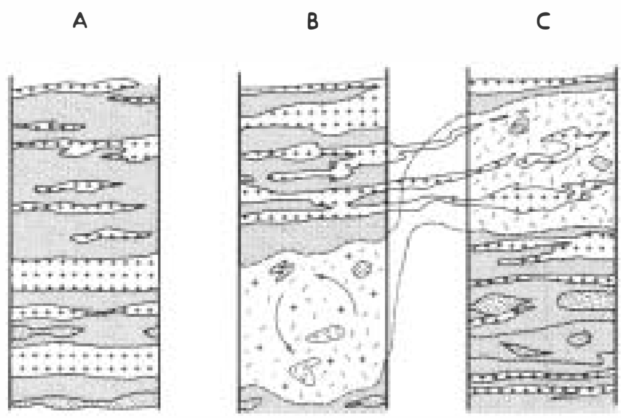

Figure 9 Schematic petrogenetic model for the generation and emplacement of the Layos Granite and associated leucogranites. (A) Development of wide migmatite zones in which pods of leucogranitic melts segregate. (B) The rheological critical melt fraction is exceeded and convective homogenisation occurs. (C) The resultant large volume of crystal-liquid mush segregates and with limited ascent within the crust develops syntectonic intrusions accompanied by segregation of leucogranitic bodies.

metamorphic climax and its restite-rich character lead to unusual mineralogical features: plagioclase is almost unzoned and does not vary in composition from the mafic to the more felsic members of the series; K-feldspar has relatively high albitic content; cordierite has low alkali and Mn content and usually contains sillimanite inclusions; biotite has high Ti and low Al^{VI} contents.

Geochemically the most remarkable characteristics are the high normative corundum values (as much as 10%) increasing in the more mafic types and the very limited variation in CaO content in the whole series.

In the light of these features, the chemical variations observed in the Layos Granite can be best explained by a restite-unmixing process between an acid pole represented by the associated minimum-temperature melt leucogranites and a restite pole constituted by the peraluminous granulites that are spatially, chemically and mineralogically associated with the Layos Granite. The source material of the Layos Granite has the chemical and isotopic characteristics of a pelitic metasediment. The high proportion of restitic material in the Layos Granite confers a relatively restricted movement capacity, resulting in a parautochthonous emplacement of this crystal-liquid mush.

The Layos Granite has contrasted petrographical and geochemical features compared to the main cordierite-bearing batholiths of the Iberian Variscan Belt. These monzogranitic batholiths usually define Gueret-type trends on an A–B plot, being more peraluminous in the more felsic varieties. We consider that this voluminous plutonism, late to post-tectonically emplaced in upper levels, has experienced considerable mobility within the crust and has to be derived from different source materials, probably more granodioritic in composition.

The scarcity of restite-rich granites such as the Layos Granite implies that dry melting of pelitic protoliths is not the usual mechanism of melt generation in this part of the Iberian Hercynian Belt.

7. Acknowledgements

We are especially grateful to Norman Snelling for his constructive critical review and for the revision of the English version of the text. We wish also to acknowledge the contributions of Alexandro Rottura, Bruce Chappell and two anonymous reviewers which greatly improved this manuscript. Microprobe analyses were performed at Oviedo University (Spain) kindly provided by L. G. Corretge. We thank Olga Fernández, Mayte Larrea and Maribel Sevillano for their collaboration in sample preparation and in ICP spectrometry. This work is financially supported by a CICYT (PB88-0117) project of the Ministerio de Educación y Ciencia and by a FPI-MEC grant to one of the authors (LB).

8. References

Andonaegui, P. 1990. *Geoquímica y geocronología de los granitoides del sur de Toledo.* Tesis doctoral, Universidad Complutense de Madrid, Spain.

Arzi, A. A. 1978. Critical phenomena in the rheology of partially melted rocks. TECTONOPHYSICS **44,** 173–89.

Barbero, L. & Villaseca, C. 1988. Gabros coroníticos en el macizo cristalino de Toledo. GEOGACETA **5,** 67–9.

Barbero, L., Villaseca, C. & Andonaegui, P. 1990. On the origin of the gabbro–tonalite–monzogranite association from Toledo area (Hercynian Iberian belt). SCHWEIZ MINERAL PETROGR MITT **7,** 209–21.

Barbey, P., Bertrand, J. M., Angoua, S. & Dautei, D. 1989. Petrology and U/Pb chronology of the Telohat migmatites (Aleksod, Central Hoggar). CONTRIB MINERAL PETROL **101,** 207–19.

Barbey, P., Macaudiere, J. & Uzenti, J. P. 1990. High-pressure dehydration melting of metapelites: evidence from migmatites of Yaoundí (Cameroon). J PETROL **31,** 401–28.

Bohlen, J. R. & Liotta, J. J. (1986). A barometer for garnet amphibolites and garnet granulites. J PETROL **27,** 1024–34.

Bowden, P., Batchelor, R. A., Chappell, B. W., Didier, J. & Lameyre, J. 1984. Petrological, geochemical and source criteria for the classification of granitic rocks: a discussion. PHYS EARTH PLANET INTERIORS **35,** 1–11.

Brandebourger, E. 1984. *Les granitoides hercyniens tardifs de la Sierra de Guadarrama (Système Central, Espagne).* Pétrographie et geochimie, These 3eme Cycle, CNRS, France.

Brändle, J. L. & Cerqueira, I. 1972. Determinación de elementos menores en rocas silicatadas por fluorescencia de rayos X. ESTUD GEOL **28,** 445–51.

Casillas, R. 1989. *Las asociaciones plutónicas tardihercínicas del sector occidental de la Sierra de Guadarrama—Sistema Central Español, (Las Navas del Marqués–San Martín de Valdeiglesias). Petrología, geoquímica, génesis y evolución.* Tesis Doctoral, Universidad Complutense de Madrid, Spain.

Casquet, C., Fuster, J. M., González Casado, J. M., Peinado, M. & Villaseca, C. 1988. Extensional tectonics and granite emplacement in the Spanish Central System. A discussion. EUROPEAN SCI FOUND (SPEC VOL), PROC 5th WORK, 65–76.

Chappell, B. W., White, A. J. R. & Wyborn, D. 1987. The importance of residual source material (restite) in granite petrogenesis. J PETROL **28,** 1111–38.

Clarke, R. G. & Lyons, J. B. 1986. Petrogenesis of the Kingsman intrusive suite: peraluminous granitoids of Western New Hampshire. J PETROL **27,** 1365–93.

Debon, F. & Le Fort, P. 1983. A chemical-mineralogical classification of common plutonic rock and associations. TRANS R SOC EDINBURGH: EARTH SCI **73,** 135–49.

Del Moro, A. 1987. Sistematica Rb/Sr di alcune magmatiti tardo-erciniche dell'area italiana. RIC SCI EDUC PERM **52,** 107–32.

Dymek, F. R. 1983. Titanium, aluminium and interlayered cation substitution in biotite from high-grade gneisses, west Greenland. AM MINERAL **68,** 880–99.

Ebadi, A. & Johannes, W. 1991. Bėginning of melting and composition of first melts in the system Qz–Ab–Or–H_2O–CO_2. CONTRIB MINERAL PETROL **106,** 286–95.

Ferry, J. M. & Spear, F. S. 1978. Experimental calibration of the partitioning of Fe and Mg between garnet and biotite. CONTRIB MINERAL PETROL **66,** 113–7.

Flood, R. H. & Shaw, S. E. 1975. A cordierite-bearing granite suite from the New England batholith. N.S.W. Australia. CONTRIB MINERAL PETROL **52,** 157–64.

Frost, B. R. & Chacko, T. 1989. The granulite uncertainty principle: limitations on thermobarometry in granulites. J GEOL **97,** 435–50.

Ganguly, J. & Saxena, S. K. 1984. Mixing properties of aluminosilicate garnets: constrains for natural and experimental data and application to geothermo-barometry. AM MINERAL **69,** 88–97.

Ghent, E. D. & Stout, M. Z. 1984. TiO_2 activity in metamorphosed pelitic and basic rocks: principles and applications to metamorphism in southeastern Canadian Cordillera. CONTRIB MINERAL PETROL **86,** 248–55.

Grapes, R. H. 1985. Melting and thermal reconstruction of pelitic xenolith, Wehr volcano, east Eifel, west Germany. J PETROL **27,** 343–96.

Green, D. & Ringwood, A. 1967. An experimental investigation of the gabbro to eclogite transformation and its petrological applications. GEOCHIM COSMOCHIM ACTA **31,** 767–833.

Gromet, L. P., Dymek, R. F., Haskin, L. A. & Korotev, R. L. 1984. The "North American Shale composite": its compilation, major and trace element characteristics. GEOCHIM COSMOCHIM ACTA **48,** 2469–82.

Hodges, K. V. & Spear, F. S. 1982. Geothermometry, geobarometry and the Al_2O_3 triple point at Mt Moosilauke, New Hampshire. AM MINERAL **67,** 1118–34.

Holdaway, M. J. & Lee, S. N. 1977. Fe–Mg cordierite stability in high-grade pelitic rocks based on experimental, theoretical and natural observations. CONTRIB MINERAL PETROL **63,** 175–98.

Ibarguchi, J. I. G. & Martínez, F. J. 1982. Petrology of garnet–cordierite–sillimanite gneisses from the El Tormes thermal Dome, Iberian Hercynian foldbelt (W Spain). CONTRIB MINERAL PETROL **80,** 14–24.

Jones, K. A. & Brown, M. 1990. High-temperature 'clockwise' P–T paths and melting in the development of regional migmatites: an example from southern Brittany, France. J MET GEOL **8,** 551–78.

Julivert, M., Fontboté, J. M., Ribeiro, A. & Conde, L. E. 1974. *Memoria explicativa del mapa tectónico de la Península Ibérica y Baleares. Escala 1 : 100,000.* I.G.M.E., Madrid, Spain.

Lavrenteva, E. V. & Perchuck, L. L. 1981. Cordierite–garnet thermometer. A collection of theses. ACAD SCI USSR **259,** 607–700.

Le Breton, N. & Thompson, A. B. 1988. Fluid-absent (dehydration) melting of biotite in metapelites in the early stages of crustal anatexis. CONTRIB MINERAL PETROL **99,** 226–37.

Martín Escorza, C. & López Martínez, J. 1978. Análisis mesoestructural en la Unidad Migmatítica de Toledo. ESTUD GEOL **34,** 34–43.

Masuda, A., Nakamura, N. & Tanaka, T. 1973. Fine structures of mutual normalized rare earth patterns of chondrites. GEOCHIM COSMOCHIM ACTA **37,** 239–48.

McRae, N. D. & Nesbitt, H. W. 1980. Partial melting of common metasedimentary rocks: a mass balance approach. CONTRIB MINERAL PETROL **75,** 21–6.

Miller, C. F. 1985. Are strongly peraluminous magmas derived from pelitic sedimentary sources? J GEOL **93,** 673–89.

Miller, C. F., Watson, E. B. & Harrison, T. M. 1988. Perspectives on the source, segregation and transport of granitoid magmas. TRANS R SOC EDINBURGH EARTH SCI **79,** 135–56.

Minster, F. J. & Allègre, C. J. 1977. Systematic use of trace elements in igneous processes. Part I: Fractional crystallization processes in volcanic suites. CONTRIB MINERAL PETROL **60,** 57–75.

Moller, P. & Muecke, G. K. 1984. Significance of europium anomalies in silicate melts and crystal melt equilibria: a re-evaluation. CONTRIB MINERAL PETROL **87,** 242–50.

Patiño, A. & Johnston, A. 1991. Phase equilibria and melt productivity in the pelitic system: implications for the origin of peraluminous granitoids and aluminous granulites. CONTRIB MINERAL PETROL **107,** 202–18.

Rottura, A., Bargossi, G. M., Caironi, V., D'Amico, C. & Maccarrone, E. 1989. Petrology and geochemistry of late-Hercynian granites from the Western Central System of the Iberian Massif. EUR J MINER **1,** 667–83.

Rottura, A., Bargossi, G. M., Caironi, V., Del Moro, A., Maccarrone, E., Macera, P., Paglionico, A. Petrini, R. Piccarreta, G. & Poli, G. 1990. Petrogenesis of contrasting Hercynian granitoids from the Calabrian Arc, southern Italy. LITHOS **24,** 97–119.

Sawyer, E. W. 1987. The role of partial melting and fractional crystallisation in determining discordant migmatite leucosome compositions. J PETROL **28,** 445–73.

Sengupta, P., Dasgupta, S. K., Bhattacharya, P. K. & Mukherjee, M. 1990. An orthopyroxene–biotite geothermometer and its application in crustal granulites and mantle derived rocks. J MET GEOL **8,** 191–8.

Speer, J. A. 1981. Petrology of cordierite- and almandine-bearing granitoid plutons of the southern Appalachian piedmont, U.S.A. CAN MINERAL **19,** 35–46.

Streckeisen, A. 1976. To each plutonic rock its proper name. EARTH SCI REV **12,** 1–13.

Thompson, R. N., Morrison, M. A., Hendry, G. L. & Parry, S. J. 1984. An assessment on the relative roles of crust and mantle magma genesis: an elemental approach. PHILOS TRANS R SOC LONDON **A310,** 549–90.

Van der Molen, I. & Paterson, M. S. 1979. Experimental deformation of partially-melted granite. CONTRIB MINERAL PETROL **70,** 299–318.

Vialette, Y., Casquet, C., Fúster, J. M., Ibarrola, E., Navidad, M., Peinado, M. & Villaseca, C. 1987. Geochronological study of orthogneisses from the Sierra de Guadarrama (Spanish Central System). N JARB MINER MH JG **H10,** 465–79.

Vielzeuf, D. 1983. The spinel and quartz associations in high grade xenoliths from Tallante (SE Spain) and their potential use in geothermometry and barometry. CONTRIB MINERAL PETROL **82,** 301–11.

Vielzeuf, D., Clemens, J. D., Pin, C. & Moinet, E. 1990. Granites, granulites and crustal evolution. *In* Vielzeuf, D. & Vidal, Ph. (eds) *Granulites and crustal evolution.* NATO ASI SCI SER C **311,** 59–85.

Vielzeuf, D. & Holloway, J. R. 1988. Experimental determination of the fluid-absent melting relations in the pelitic system. Consequences for crustal differentiation. CONTRIB MINERAL PETROL **98,** 257–76.

Villaseca, C. 1983. *Evolución metamórfica del sector centro-septentrional de la Sierra de Guadarrama.* Tesis Doctoral 216/84, Universidad Complutense de Madrid, Spain.

Villaseca, C. & Barbero, L. (in press). Los granates de rocas metapelíticas de la región central española: implicaciones en el origen de granates en granitoides. GEOGACETA (in press).

Vry, J. K., Brown, E. B. & Valley, J. W. 1990. Cordierite volatile content and the role of CO_2 in high-grade metamorphism. AM MINERAL **75,** 71–88.

Watson, E. B. 1987. The role of accessory minerals in granitoid geochemistry. 1ST HUTTON SYMP ABSTR, 19–21.

Wells, P. R. A. 1977. Pyroxene thermometry in simple and complex systems. CONTRIB MINERAL PETROL **62,** 129–39.

Whalen, J. B. & Chappell, B. W. 1988. Opaque mineralogy and mafic mineral chemistry of I- and S-type granites of the Lachlan fold belt, southern Australia. AM MINERAL **73,** 281–96.

White, A. J. R. & Chappell, B. W. 1987. Some supracrustal (S-type) granites of the Lachlan Fold Belt. TRANS R SOC EDINBURGH EARTH SCI **79,** 169–81.

Wickham, S. M. 1987a. Crustal anatexis and granite petrogenesis during low pressure regional metamorphism in the Trois Seigneurs massif, Pyrenees, France. J PETROL **28,** 127–69.

Wickham, S. M. 1987b. The segregation and emplacement of granitic magmas. J GEOL SOC LONDON **144,** 281–97.

Wildberg, H. G. H., Bischoff, L. & Baumann, A. 1989. U–Pb ages of zircons from meta-igneous and metasedimentary rocks of the Sierra de Guadarrama: implications for the Central Iberian crustal evolution. CONTRIB MINERAL PETROL **103,** 253–62.

L. BARBERO and C. VILLASECA, Dpto. Petrología y Geoquímica, Fac. C.C. Geológicas, Universidad Complutense, 28040 Madrid, Spain.